Journal of Sustainable Metallurgy
https://doi.org/10.1007/s40831-024-00815-4

RESEARCH ARTICLE

Conversion of Lithium Chloride into Lithium Hydroxide Using a Two-Step Solvent Extraction Process in an Agitated Kühni Column

Nand Peeters[1] · Sofía Riaño[1] · Koen Binnemans[1]

Received: 10 November 2023 / Accepted: 13 March 2024

Abstract

A significant consequence of the green transition is the growing demand of lithium-ion batteries (LIBs), as they are essential for electrical vehicles. In turn, the demand for the raw materials that are needed to produce LIBs is increasing. A common LIB cathode type for electrical cars is lithium nickel manganese cobalt oxide (NMC). Since cobalt is currently considered as a critical raw material, nickel-rich NMC cathodes are now designed with lower cobalt contents. The synthesis of these new NMC types requires LiOH instead of Li_2CO_3, which was used for Co-richer NMC materials in the past. Most production routes of LiOH start from Li_2CO_3 or Li_2SO_4. However, LiCl could also be a potential precursor for LiOH, as it could be obtained from various lithium sources. A two-step solvent extraction process (SX) was developed for direct conversion of LiCl into LiOH, using a phenol (butylhydroxytoluene or BHT) and a mixture of quaternary ammonium chlorides (Aliquat 336) in an aliphatic diluent (Shellsol D70) as the solvent. The SX process was validated in counter-current mode using a rotary agitated Kühni extraction column. The use of a column instead of mixer-settlers reduced the CO_2 uptake by the final product (LiOH), which prevented the partial conversion of LiOH to Li_2CO_3. A total of 75 L of LiCl feed solution was processed in the Kühni column to obtain a solution of LiOH with a final purity of more than 99.95%, at a yield of 96%.

Graphical Abstract

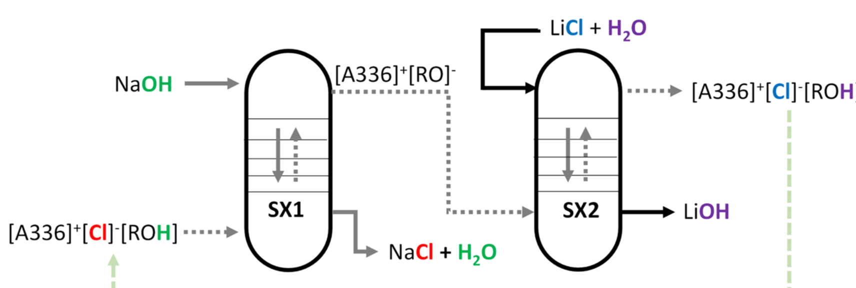

Keywords Hydrometallurgy · Liquid–liquid extraction · Lithium · Solvent extraction

Introduction

Lithium nickel manganese cobalt oxide ($LiNi_xMn_yCo_{1-x-y}O_2$, NMC) is a commonly used cathode material in Li-ion batteries (LIBs) [1, 2]. Over the years, there has been a shift from cobalt-rich NMC types (e.g., NMC 111), to nickel-rich types, such as NMC 811 and NMC 622. Whereas cobalt-rich NMC can be synthesized using Li_2CO_3 as a lithium source, nickel-rich NMC requires the use of LiOH as a precursor. This allows the synthesis to occur at lower temperatures,

The contributing editor for this article was Yongxiang Yang.

Koen Binnemans
Koen.Binnemans@kuleuven.be

[1] Department of Chemistry, KU Leuven, Celestijnenlaan 200F, P.O. Box 2404, 3001 Leuven, Belgium

Published online: 08 April 2024

hereby avoiding damages to the crystal structure and preventing nickel from oxidizing in the oxide lattice [3]. However, the current focus is mainly on the recovery of lithium by precipitating lithium from solution as Li_2CO_3 with the addition of soda ash, Na_2CO_3 [4–6]. As the market for NMC 811 and 622 is increasing, more mining industries are trying to produce LiOH instead of Li_2CO_3, with the commercial form being crystalline lithium hydroxide monohydrate ($LiOH \cdot H_2O$) [7]. LiOH can be produced starting from Li_2CO_3 by reaction with $Ca(OH)_2$ or by reacting Li_2SO_4 with NaOH or $Ba(OH)_2$, [3, 7, 8].

In many novel lithium recovery processes, such as those based on direct lithium extraction from primary lithium resources [9], but also in many LIBs recycling processes [10, 11], lithium is recovered in the form of LiCl. A process for direct transformation of LiCl into $LiOH \cdot H_2O$, bypassing the Li_2CO_3 intermediate, would be advantageous from an economical and environmental point of view because this reduces the number of processing steps, leads to the consumption of less chemicals, and generates less waste [8]. Recently, our research group has developed a method that purifies LiCl to battery-grade by using organic solvents [12].

Additionally, we developed a new method that converts battery-grade LiCl into LiOH by solvent extraction (SX) (Fig. 1) [3]. Here, the organic phase consisting of the quaternary ammonium salts Aliquat 336 ($[A336]^+[Cl]^-$) and 2,6-di-*tert*-butylphenol is contacted with 2 mol L^{-1} NaOH. This initial SX step (SX1) deprotonates the phenol and transfers the chloride anion of $[A336]^+[Cl]^-$ to the aqueous phase. After extraction, NaOH is converted into NaCl in the aqueous phase and the cation of $[A336]^+$ recombines with the anionic phenolate in the organic phase. The latter phase is then contacted with 1.6 mol L^{-1} of battery-grade LiCl in the subsequent step (SX2). The phenolate in the organic phase gets then re-protonated by water, forming OH^- in the aqueous phase. The Cl^- counter-anion of LiCl is then transferred to the organic phase to maintain the electric neutrality [3]. Thus, after extraction, $[A336]^+[Cl]^-$ and the phenol in the organic phase are regenerated for the subsequent cycle and Li^+ combines with OH^- in the aqueous phase. This process was successfully demonstrated in counter-current coupled mixer-settlers, reaching a conversion of LiOH of 97.7% and losses up to 7% of the final product ($LiOH \cdot H_2O$)

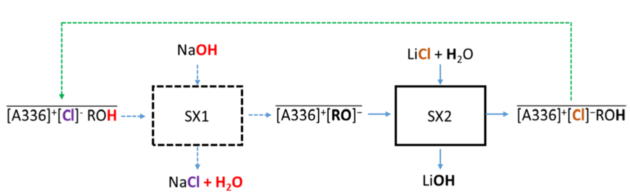

Fig. 1 Schematic overview of the two-step SX process for the conversion of LiCl into LiOH [3]

due to partial conversion of LiOH into Li_2CO_3 by reaction with CO_2 in the atmosphere.

Losses in this process due to conversion of LiOH into Li_2CO_3 could be avoided by using more closed contactors instead of open mixer-settlers. Compared to mixer-settlers, column-type extractors can be almost completely sealed, making them better suited for air-sensitive systems. Columns are cylindrical contactors that require large head room instead of the large foot print of mixer-settlers. While mixer-settlers have discrete stages (*i.e.*, there is phase disengagement after each stage), columns are considered as differential equipment, and the separation only takes place at the top and bottom of the column. The continuous phase (where the other phase is going to be in dispersed) is the phase that is used to initially fill the column and often the one that is pumped-in at a higher flow rate. In an agitated column, a stirrer is responsible for the mechanical agitation and its shape is comparable to a rotating disk [13–15].

In this paper, the process developed in our group is further improved and tested in counter-current mode in a rotary agitated Kühni extraction column. The efficiency of BHT (butylhydroxytoluene) as phenol is compared with the originally used 2,6-di-*tert*-butylphenol, since BHT is cheaper and more accessible. McCabe–Thiele diagrams are constructed, the contact times are optimized and the settling speeds are determined. The entire counter-current SX process to convert LiCl into LiOH is carried out in counter-current mode in a Kühni column. Advantages and disadvantages on the use of columns instead of mixer-settlers are discussed.

Experimental

Chemicals

Lithium chloride (> 99%), sulfuric acid (> 95%), sodium hydroxide (> 98%), sodium chloride (> 99%), tris(hydroxymethyl)aminomethane (< 99%), and methanol (> 99.8%) were purchased from Thermo Fisher Scientific (Geel, Belgium). Aliquat 336 (A336, $[A336]^+[Cl]^-$, a commercial mixture of quaternary ammonium chlorides, 90%) and Trition X-100 (> 99%) were purchased from Sigma-Aldrich (Overijse, Belgium), 2,6-di-*tert*-butyl-4-methylphenol (butylhydroxytoluene, butylated toluene, BHT, 99%) was bought from Acros Organics (Geel, Belgium), and the aliphatic diluent (Shellsol D70, C11-C14 hydrocarbons) was obtained from Shell Global Solutions (Amsterdam, The Netherlands). The titrants $AgNO_3$ and HCl were purchased from Chem Lab (Zedelgem, Belgium) and aqueous ammonia solution (25%) was bought from VWR International (Leuven, Belgium). Ultrapure water (18.2 MΩ cm) was generated by a Millipore MilliQ Reference A + system. All chemicals were used as received, without any further purification.

Instrumentation

The lithium concentration was determined by inductively coupled plasma-optical emission spectroscopy (ICP-OES), using a PerkinElmer Avio500 spectrometer equipped with a Meinhard Low-Flow Nebulizer, baffled cyclonic spray chamber, 1.2 mm inner diameter alumina injector, and Perkin-Elmer Hybrid XLT torch. The ionization interference of lithium was minimized by shortening the detector distance. Samples were diluted 500 times. The chloride concentration in the aqueous phase was determined by an automated argentometric titration using a combined silver ring electrode (Mettler-Toledo DMi141-SC) in combination with an automated titrator (Mettler-Toledo T5 Excellence) and an autosampler (InMotion Autosampler Flex). The titrant (0.05 mol L^{-1} $AgNO_3$) was calibrated by weighing approximately 10 mg of dry NaCl in a titration cup and adding *ca*. 40 mL of 0.02 mol L^{-1} H_2SO_4 and 2 mL of aqueous 5 vol% Triton X-100 solution. The electrode was first washed with a 0.5 wt% NH_3 solution followed by a 0.02 mol L^{-1} H_2SO_4 solution. The hydroxide concentration in the aqueous phase was determined by an automated potentiometric titration using a combined glass pH electrode (Mettler-Toledo DMi111-SC) in combination with an automated titrator (Mettler-Toledo T5 Excellence) and autosampler (InMotion Autosampler Flex). The pH electrode was rinsed with MilliQ water. The titrant (0.1 mol L^{-1} HCl) was calibrated by weighing approximately 50 mg of dry tris(hydroxymethyl) aminomethane in a titration cup and adding *ca*. 40 mL of milliQ water [3]. GC–MS measurements were done on a PerkinElmer Autosystem XL/Turbomass Kolom equipped with a PerkinElmer column of 60 cm length and 0.25 mm diameter, coating Perkin 5MS and film thickness of 1 µm. The operational parameters were: injection volume = 1 µL; oven temperature = 45–230 °C; injection temperature = 220 °C; source temperature = 200 °C; helium pressure on the carrier = 15 psi; split flow = 15 mL min^{-1} [16].

Solvent Extraction 1 (SX1)

The solvent was prepared by weighing equimolar amounts (n:n = 1) of $[A336]^+[Cl]^-$ and BHT in a beaker and adding 45 wt% of an aliphatic diluent (Shellsol D70). This solvent can be represented by $\overline{[A336]^+[Cl]^-BHT}$. Batch-scale experiments were executed by transferring volumes of 2 mol L^{-1} NaOH and the solvent at the chosen O:A ratio into 4 mL glass vials. A magnetic stirring bar was inserted and the vials were sealed with screw caps containing a septum. Extraction was then done by placing the vial on a magnetic stirring plate and stirring at 900 rpm for 30 min. The aqueous and organic phases were sampled for further analysis. If an inert atmosphere was required, nitrogen gas was initially flushed through the aqueous and organic phase and the empty vial, followed by bubbling nitrogen gas via the septum cap through the vial during mixing. Samples were taken with a needle syringe via the septum for further analysis. The sample vials were centrifuged for 5 min at 5000 rpm. GC–MS samples were taken by transferring 50 µL into a GC vial and adding 950 µL of methanol. The chloride content of the aqueous phases (*i.e.,* $[Cl^-]_{aq}$) was determined by an argentometric titration by transferring an aliquot of about 275 mg into a glass titration cup. Subsequently, approximately 40 mL of milliQ water was added together with 2 mL of aqueous 5 vol% Triton X-100. The pH was adjusted to 4.5–5.0 by inserting a pH -sensor and adding amounts of H_2SO_4 (and NaOH if needed) in concentration ranges of 0.01–6 mol L^{-1} while stirring with a magnetic bar. The conversion rate of SX1 (*%-SX1*) was calculated with Eq. (1) [3]:

$$\% - SX1 = \frac{\left([Cl^-]_{aq} \cdot V_{aq}\right)}{\left([Cl^-]_{i,\,org} \cdot V_{org}\right)} \cdot 100 \tag{1}$$

Here, V_{aq} and V_{org} are the volumes of the aqueous and organic phases, $[Cl^-]_{i,org}$ is the initial chloride concentration in the organic phase that was calculated with the weighed amount of $[A336]^+[Cl]^-$, the purity of $[A336]^+[Cl]^-$, the average molar mass of $[A336]^+[Cl]^-$, and the entire volume of $\overline{[A336]^+[Cl]^-BHT}$.

Solvent Extraction 2 (SX2)

The organic phase after SX1 (*i.e.,* $\overline{[A336]^+[RO]^-}$) and 1.6 mol L^{-1} battery-grade LiCl were used for SX2 via the same extraction and GC–MS sampling procedures as described above. Batch-scale experiments were here always executed under nitrogen atmosphere as mentioned in the previous section. The hydroxide content was determined with an acid–base titration by transferring an aliquot of about 550 mg of the sample via the septum cap of the vial with a needle-syringe into a titration cup and adding immediately *circa* 40 mL of nitrogen-flushed milliQ water. A frit was attached on a tube and the other end of the tube was attached to one side of a valve. A balloon filled with nitrogen gas was attached to the other side of the valve. The frit was inserted in one of the inlets of the autosampler, providing a constant nitrogen gas stream over the cups during the automated titrations. The conversion rate of SX2 (*%-SX2*) was calculated with Eq. (2) [3]:

$$\% - SX2 = \frac{[LiOH]_{eq}}{[LiCl]_i} \cdot 100 \tag{2}$$

Here, $[LiOH]_{eq}$ and $[LiCl]_i$ are, respectively, the LiOH concentration after extraction (calculated via determination of hydroxide concentration with acid–base titration) and the initial LiCl concentration (determined by an argentometric titration, as described above).

Physical Properties of SX Streams

The density and viscosity of all streams of both SX processes were determined with an automatic rolling-ball viscosity meter Lovis (Model 2000 M/ME), with a density measuring module (MA 4500 ME, Anton Paar GmbH, Graz, Austria). The settling speeds were determined by transferring the organic and aqueous phases, each at a minimum volume of 50 mL, into a high glass beaker of 250 mL (12.3 × 7.0 × 6.8 cm) at the optimized O:A. The distance of both phases to the interphase was measured with a caliper and a rotating disk impeller was used to mix both phases. If the impeller was located in the upper organic phase, mixing ensured an organic phase continuity and vice versa for aqueous-phase continuity. After stirring for 30 min, mixing was stopped and the time until phase disengagement was measured.

Agitated Column Experiments

Stock solutions of 75 L of a 2 mol L^{-1} NaOH, 0.65 mol L^{-1} $[A336]^+[Cl]^-BHT$, and 1.6 mol L^{-1} LiCl were prepared. The two SX operations were carried out in a mechanically agitated, borosilicate glass extraction column, type Kühni ECR 32 (Sulzer, Switzerland). The column consisted of five sections with an inner diameter of 32 mm, and the active volume was 0.9 L when all the five column sections were used. The wetted internals (rotor and stator) were made of PEEK and agitation in each stage was achieved with a turbine agitator on top of the column. Two settlers were located at each end of the column. Both aqueous and organic phases were pumped using a Masterflex L/S Precision Variable-Speed Console Drive equipped with Easy-Load pump heads. To ensure aqueous-continuous conditions, the column was loaded by filling it first with the aqueous phase and afterward pumping the organic phase. The aqueous phase was then pumped at a higher flow rate to ensure an aqueous-phase continuity. The opposite operation was done to ensure organic-continuous conditions. For SX1, the flow of the organic and aqueous phases corresponded to 22 and 53 mL min^{-1} (O:A ratio = 1:2), respectively. For SX2, the flow of the organic and aqueous phases corresponded to 92 and 23 mL min^{-1} (O:A ratio = 4:1), respectively. The initial stirring speed for both SX corresponded to 500 rpm. The interphase level was kept in the middle of the top settler with the help of a siphon. Samples were taken via the nozzles of each section of the column [15].

Results and Discussion

McCabe–Thiele Diagrams for SX1 and SX2

Information on the theoretical number of stages of a liquid–liquid extraction process can be derived from a McCabe–Thiele diagrams. The McCabe–Thiele diagrams for SX1 and SX2 of BHT mixed with $[A336]^+[Cl]^-$ in the aliphatic diluent Shellsol D70 $\left([A336]^+[Cl]^-BHT\right)$ are illustrated in Fig. 2. Comparison with the McCabe–Thiele diagrams of Nguyen et al. confirms that the phenols BHT and 2,6-di-*tert*-butylphenol yield similar conversion rates [3]. The diagrams estimate that SX1 requires three mixer-settler stages at O:A = 1:2, while SX2 requires five stages at O:A = 4:1. These observations are similar to the results obtained by Nguyen et al., but it has to be noticed that they

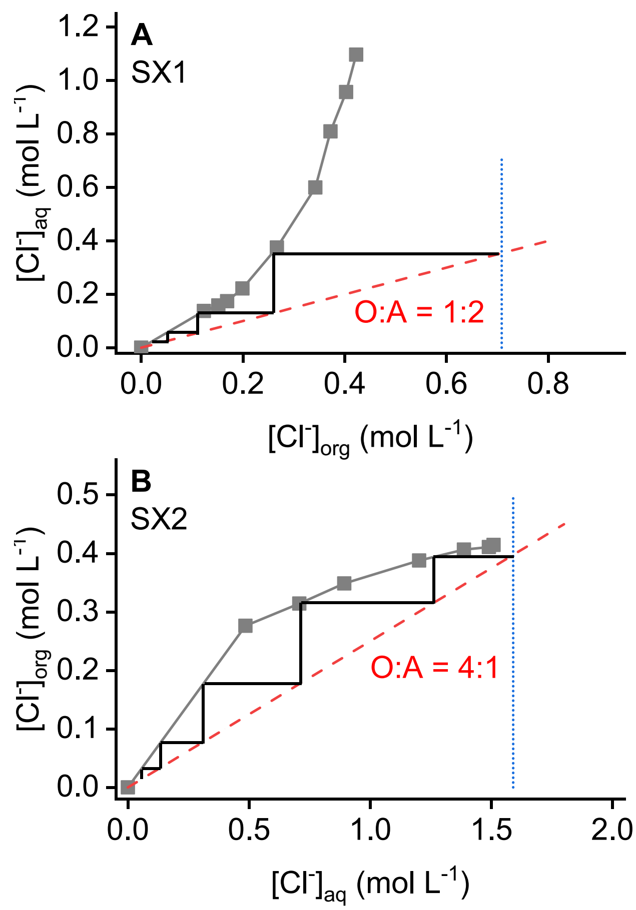

Fig. 2 McCabe–Thiele diagrams of SX1 (**A**) and SX2 (**B**). SX1 Organic phase: 0.65 M $[A336]^+[Cl]^-$ and BHT (molar ratio = 1:1) in Shellsol D70; Aqueous phase: 2.0 mol L^{-1} NaOH. SX2 Organic phase: 0.65 M $[A336]^+[OR]^-$ in Shellsol D70; Aqueous phase: 1.6 mol L^{-1} LiCl. All diagrams were constructed from O:A = 1:5 to 5:1; 23 °C and contact time = 30 min

Table 1 Physical properties of the organic and aqueous phases before and after each SX unit and settling velocities

	Stream	ρ (g mL^{-1})	η (mPa s)	$v_{settling}$ (mm s^{-1})	Phase continuity
SX1	$[A336]^+[Cl]^-ROH$	0.85	24.39	0.56	Aqueous
	NaOH	1.08	1.40		
	$[A336]^+[OR]^-$	0.85	38.91	0.12	Organic
	NaCl	1.08	1.30		
SX2	$[A336]^+[OR]^-$	0.85	38.91	0.14	Aqueous
	LiCl	1.03	1.02		
	$[A336]^+[Cl]^-ROH$	0.86	23.28	0.81	Organic
	LiOH	1.04	1.25		

All measurements were made at 23 °C

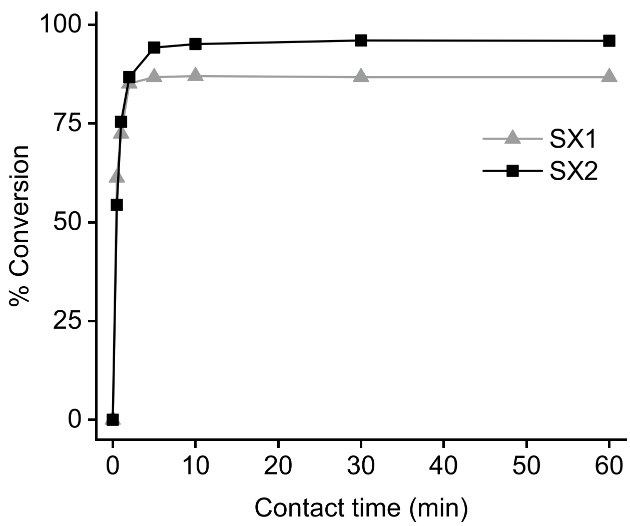

Fig. 3 Optimization of the contact time for both SX processes. SX1: O:A = 1:2, Organic phase: 0.65 M $[A336]^+[Cl]^-$ and BHT (molar ratio = 1:1) in Shellsol D70; Aqueous phase: 2.0 mol L^{-1} NaOH. SX2: O:A = 4:1 Organic phase: 0.65 M $[A336]^+[OR]^-$ in Shellsol D70; Aqueous phase: 1.6 mol L^{-1} LiCl. All experiments were done at 23 °C

carried out the SX2 step using an O:A = 3:1 (see online supplementary material Fig. S1) [3].

Viscosities, Densities, Contact Times, and Settling Velocities

The physical properties of fluids are crucial to predict their behavior in continuous processes. Furthermore, the contact time and settling speed of each SX operation can indicate whether a column type of extractor is suited. The physical properties and settling velocities of the process presented in this work are given in Table 1, while the contact time optimization is shown in Fig. 3. The contact times that were required to attain equilibrium were two minutes for SX1 and three minutes for SX2. Although columns are often preferred for slow extractions, they are also suitable for solvent extraction processes with fast extraction rates [13–15].

Table 2 Flow rates of both phases and stirring speed used to operate SX1 and SX2 through an agitated column

	Aqueous flow (mL min^{-1})	Organic flow (mL min^{-1})	Stirring speed (rpm)
SX1	53	22	500
SX2	23	92	400

All operations were performed at room temperature

At first sight, the density differences are similar to that between water and toluene, indicating that any extractor could be suitable [17]. In cases where one of the phases is highly viscous (≥ 180 mPa s at 21 °C), mixer-settlers are usually preferred, but it must be emphasized that the choice of a contactor depends on several factors [18, 19]. The viscosities in Table 1 are low, making the Kühni column suitable for the extraction. In order to maintain the O:A ratios of 1:2 for SX1 and 4:1 for SX2 in the Kühni column, the aqueous phase should be pumped twice as fast as the organic one during SX1 and the organic four times as fast as the aqueous during SX2. This approach will ensure, respectively, an aqueous and organic phase continuity, which are corresponding to the fastest settling velocities as shown in Table 1.

Conversion of LiCl into LiOH in a Kühni Column

Both SX processes were ran through a rotary agitated Kühni column with the main objective to circumvent CO_2 adsorption and avoid the formation of stable emulsions. The flow rates and stirring speed of the mixer are given in Table 2, and the agitated column with its five column heights is shown in Fig. 4.

The concentration profile and conversion of both processes over time and for each column height are given in Fig. 5. For SX1, the chloride concentration in the organic phase decreased when passing through the column and leveled off after *ca.* 3 h of operation time, reaching a maximum conversion of 86.5%. For SX2, the LiCl concentration in the aqueous phase decreased from the top to the bottom of the

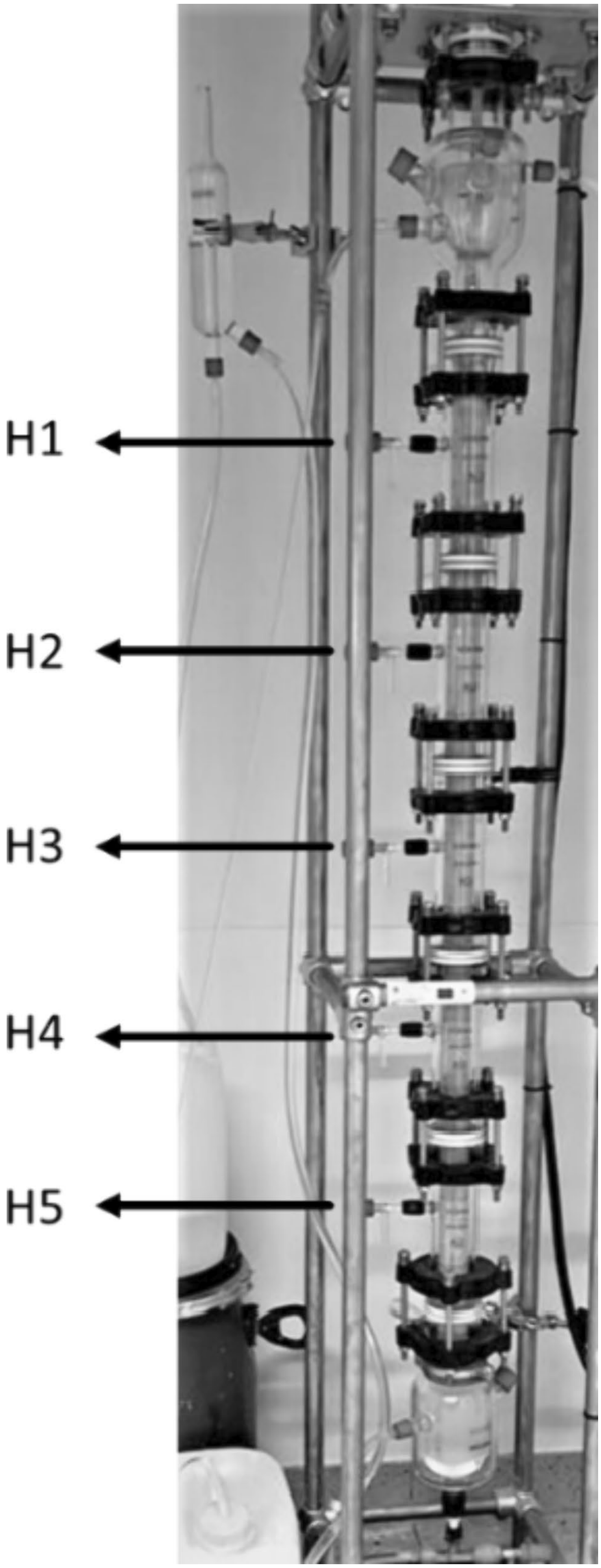

Fig. 4 The Kühni column with five column heights used for the conversion of LiCl into LiOH. Hn ($n = 1, 2\ldots$) denotes the sampling points of each one of the sections of the column

column. The decrease settled after about 3.5 h of operation time, reaching a maximum conversion of 96.2%.

No formation of stable emulsion or crud was observed during the operations, but flooding of the column was noticed for both SX1 and SX2. Flooding occurs when a phase cannot be dispersed any further into the continuous phase. The dispersed phase gets then accumulated at different column heights, preventing it to migrate upwards or downwards in the column, hereby reducing the efficiency of the extraction [17]. This unwanted phenomenon can be detected early by sampling from each nozzle every 30 to 60 min. After sampling, the phases are centrifuged to speed phase separation and the O:A should be constant. An increase in the volume of the dispersed phase indicates that flooding may be about to occur and preventive measures should be taken, such as a reduction of the stirring speed and/or the flow rates. An example of an indication for flooding is given in the online supplementary material, Fig. S2. When flooding was detected, it was mitigated by decreasing the flow rates of both phases and the stirring speed. Once the system became stable again, the flow rates were reduced to values that were 25% lower than the initial value that was applied before flooding took place.

Acid–base titration of the aqueous outlets of SX2 can detect the presence of H_2CO_3 and hence possible uptake of CO_2 by LiOH. All collected samples showed no uptake of CO_2 (see online supplementary material, Fig. S3). Hence, the agitated column enabled the successful conversion of LiCl into LiOH, without formation of significant amount of Li_2CO_3. LiOH can be precipitated from the converted solution as $LiOH \cdot H_2O$ by evaporation of water or via antisolvent precipitation, as described by Nguyen et al. [3].

Oxidation of BHT

Although Fig. 5 confirms a successful conversion, it is important to mention that BHT is prone to oxidation reactions during the process. This was noticed by the color change of the organic phase from light yellow to dark purple over time (Fig. 7). Comparison of the GC–MS chromatograms of the organic phases after SX1 and SX2 with that of the initial fresh solvent (see Fig. 6) confirmed the presence of the oxidation product of BHT. This compound was only present after both SX1 and SX2 operations and not in the freshly prepared initial solvent. The antioxidant properties of BHT cause its strong affinity for free oxygen radicals from the air, resulting in its oxidation [20, 21]. The oxidation product is a dye and is therefore responsible for the intense purple color [22]. In batch scale, this reaction could be suppressed by first flushing nitrogen gas through the extraction vials and through both phases, followed by flushing nitrogen gas through the vials while mixing. The results in Fig. 7 show that both SX1 and SX2 suffer from this side reaction

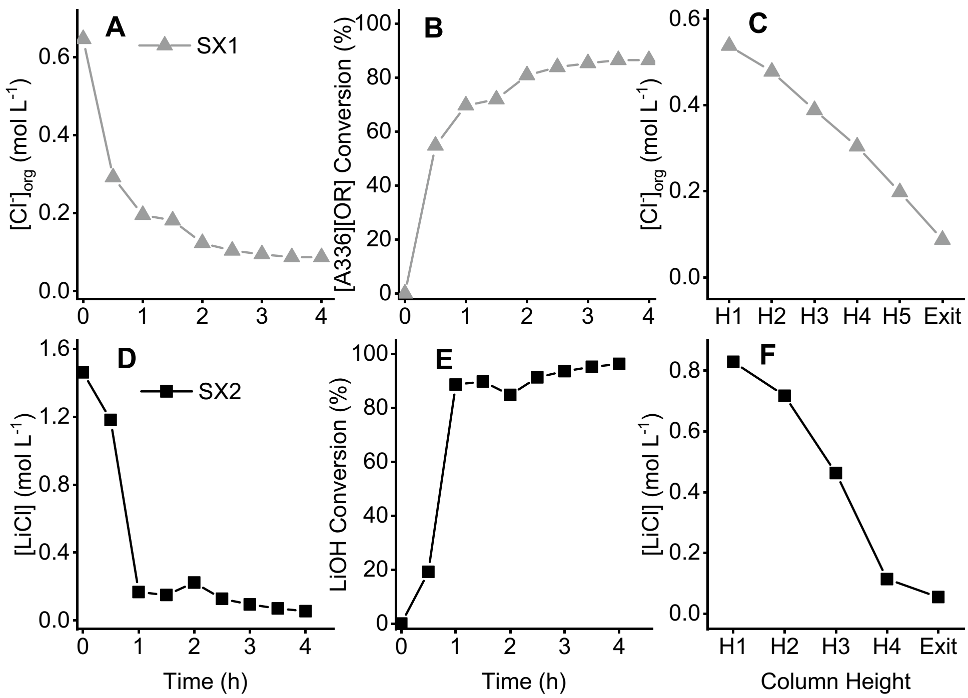

Fig. 5 Concentration profiles over time (**A** and **D**), conversions (**B** and **E**) over time and concentration profile per column height (**C** and **F**) of SX1 (above) and SX2 (below). Note that one height of the five column heights had to be repaired during operation of SX2

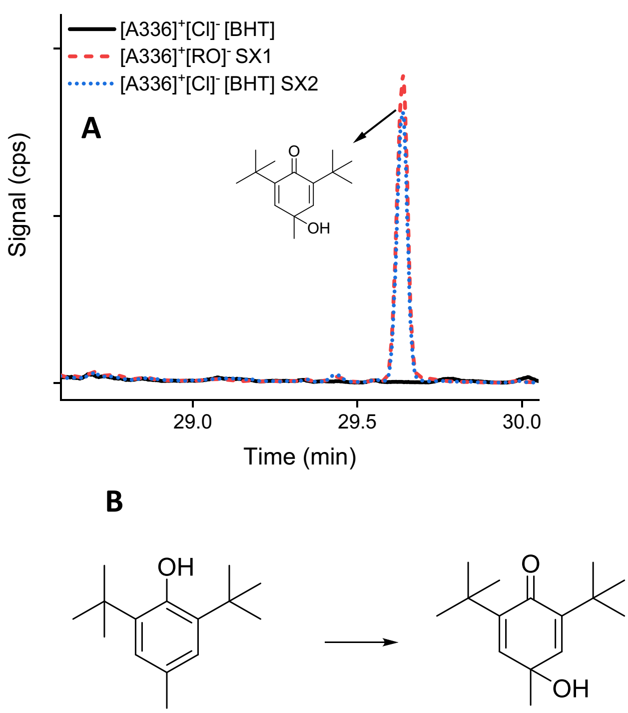

Fig. 6 Comparison of the GC–MS chromatograms of the initial organic phase with the ones after SX1 and SX2 (**A**) and the decomposition reaction of BHT (**B**)

and that an inert atmosphere could suppress these decomposition products. However, working under inert atmosphere is less straightforward at continuous scale. Although the conversion rates of SX1 and SX2 were not influenced by the antioxidant activity of BHT, it has to be noticed that this side reaction will cause conversion problems in the long-term. This is because part of the phenol will be lost in each cycle, impeding the regeneration of $[A336]^+[Cl]^-BHT$. It is therefore essential to search for an alternative phenol that does not have antioxidant properties and still gives high conversion yields. Furthermore, the mutual miscibility (aqueous phase in organic phase and vice versa) should be determined before applying the process at larger scale. The water content in the organic phase could be determined by a Karl Fischer titration, the organic content in the aqueous phase could be determined by quantitative ^{13}C nuclear magnetic resonance spectroscopy (qNMR).

Conclusion

An agitated Kühni column was found to be a suitable contactor for the successful conversion of LiCl into LiOH via the two-step solvent extraction process described in this paper. The maximum conversion rates achieved for the two steps SX1 and SX2 were similar to the ones previously reported by our group when mixer-settlers were used as contactor for the continuous counter-current extraction process [3]. In contrast to the mixer-settlers, the column minimizes the contact of the phases with air and the stirring is less intense, so that there is no partial conversion of LiOH into Li_2CO_3 by reaction with CO_2 in the air. Both SX processes were run only once through the column, without further optimization,

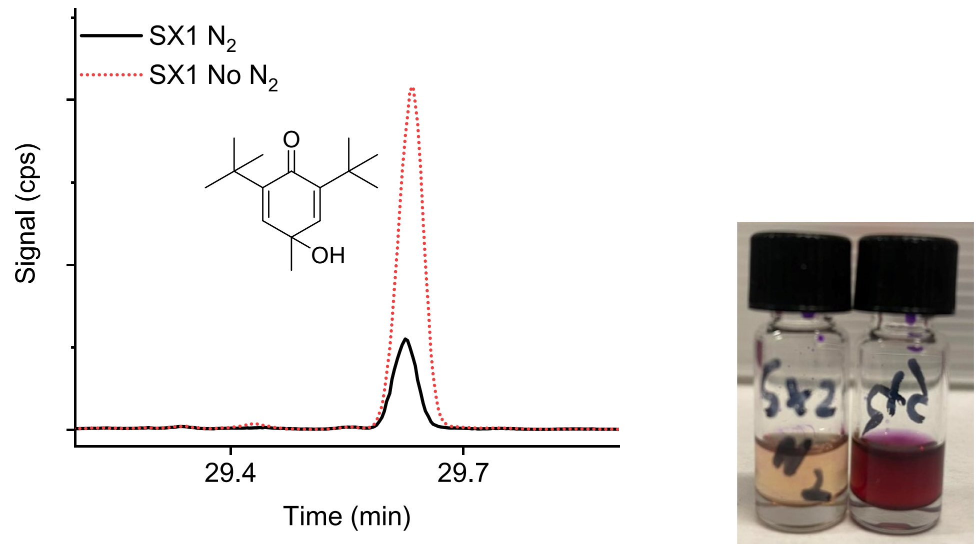

Fig. 7 Comparison of GC–MS chromatograms of the organic phases after SX1 that show the influence of nitrogen gas bubbling (left) and the influence of nitrogen gas bubbling on the color of the organic phases after SX2 (right)

which should be done in future research to improve the process. For example, fine-tuning of the flow rates and the stirring speed could further enhance the stage efficiency, followed by determining the minimum number of column heights that are required to ensure maximum conversion. The cheaper and more readily available phenol BHT showed similar conversion rates as analogous compound 2,6-di-*tert*-butylphenol described in previous study [3]. Unfortunately, BHT suffers from side reactions with free radicals due to its antioxidant properties, which will affect the long-term recyclability of the organic phase. Working under a more inert atmosphere can reduce this undesired reaction, for example, by flushing with nitrogen gas. Although we demonstrated that the purity of LiOH can be increased by using an agitated column instead of mixer-settlers, there is still room for improvement and the search for more stable systems continues.

Supplementary Information The online version contains supplementary material available at https://doi.org/10.1007/s40831-024-00815-4.

Acknowledgements This research has received funding from the Research Foundation Flanders (FWO) under Grant Agreement S008621N as part of ERA-NET Cofund on Raw Materials (ERA-MIN3) under the European Union's Framework Programme for Research and Innovation H2020 in the project ACROBAT—Advance Critical Raw Materials Recycling From Spent LFP Batteries.The authors thank Christine Wouters for the support in the GC/MS analysis.

Declarations

Conflict of interest There is no conflict to declare.

References

1. Iglesias-Émbil M, Valero A, Ortego A et al (2020) Resources, conservation & recycling raw material use in a battery electric car—a thermodynamic rarity assessment. Resour Conserv Recycl 158:1–11. https://doi.org/10.1016/j.resconrec.2020.104820
2. Barbosa A, Junior B, Martins LS et al (2021) Electric car battery: an overview on global demand, recycling and future approaches towards sustainability. J Environ Manag 295:1–16. https://doi.org/10.1016/j.jenvman.2021.113091
3. Nguyen VT, Deferm C, Cayten W et al (2023) Conversion of lithium chloride into lithium hydroxide by solvent extraction. J Sustain Metall 9:107–122. https://doi.org/10.1007/s40831-022-00629-2
4. Peng C, Liu F, Wang Z et al (2019) Selective extraction of lithium (Li) and preparation of battery grade lithium carbonate (Li_2CO_3) from spent Li-ion batteries in nitrate system. J Power Sources 415:179–188. https://doi.org/10.1016/j.jpowsour.2019.01.072
5. Chen WS, Ho HJ (2018) Recovery of valuable metals from lithium-ion batteries NMC cathode waste materials by hydrometallurgical methods. Metals 8:1–16. https://doi.org/10.3390/met8050321
6. Nguyen VT, Lee JC, Jeong J et al (2014) Selective recovery of cobalt, nickel and lithium from sulfate leachate of cathode scrap of Li-ion batteries using liquid-liquid extraction. Met Mater Int 20:357–365. https://doi.org/10.1007/s12540-014-1016-y
7. Liu H, Azimi G (2022) Production of battery grade lithium hydroxide monohydrate using barium hydroxide causticizing agent. Resour Conserv Recycl 179:1–10. https://doi.org/10.1016/j.resconrec.2021.106115
8. Dahlkamp JM, Quintero C, Videla Á, Rojas R (2023) Production processes for LiOH—a review. Hydrometallurgy 135639:1–54. https://doi.org/10.1016/j.hydromet.2023.106217

9. Vera ML, Torres WR, Galli CI et al (2023) Environmental impact of direct lithium extraction from brines. Nat Rev Earth Environ 4:149–165. https://doi.org/10.1038/s43017-022-00387-5
10. Heo J, Jones PT, Blanpain B, Guo M (2023) Chlorination roasting of li-bearing minerals and slags: combined evaluation of lithium recovery ratio and lithium chloride product purity. J Sustain Metall 9:1353–1362. https://doi.org/10.1007/s40831-023-00729-7
11. Partinen J, Halli P, Wilson BP, Lundström M (2023) The impact of chlorides on NMC leaching in hydrometallurgical battery recycling. Miner Eng 202:1–11. https://doi.org/10.1016/j.mineng.2023.108244
12. Avdibegović D, Nguyen VT, Binnemans K (2022) One-step solvometallurgical process for purification of lithium chloride to battery grade. J Sustain Metall 8:893–899. https://doi.org/10.1007/s40831-022-00540-w
13. Vancas MF (2003) Pulsed column and mixer-settler applications in solvent extraction. JOM 55:43–45. https://doi.org/10.1007/s11837-003-0124-9
14. Zhang J, Zhao B, Schreiner B (2011) Separation hydrometallurgy of rare earth elements. Springer, Cham
15. Rodrigues IR, Deferm C, Binnemans K, Riaño S (2022) Separation of cobalt and nickel via solvent extraction with Cyanex-272: batch experiments and comparison of mixer-settlers and an agitated column as contactors for continuous counter-current extraction. Sep Purif Technol 296:1–10. https://doi.org/10.1016/j.seppur.2022.121326
16. Peeters N, Janssens K, de Vos D et al (2022) Choline chloride–ethylene glycol based deep-eutectic solvents as lixiviants for cobalt recovery from lithium-ion battery cathode materials: are these solvents really green in high-temperature processes? Green Chem 24:6685–6695. https://doi.org/10.1039/d2gc02075k
17. Torab-mostaedi M, Safdari J, Ali M (2009) Chemical engineering and processing : process intensification flooding characteristics in a Hanson mixer-settler extraction column. Chem Eng Process Process Intensif 48:1249–1254. https://doi.org/10.1016/j.cep.2009.05.003
18. Riaño S, Sobekova Foltova S, Binnemans K (2020) Separation of neodymium and dysprosium by with neutral extractants: batch and mixer-settler. RSC Adv 10:307–316. https://doi.org/10.1039/c9ra08996a
19. Vereycken W, Van Gerven T, Binnemans K (2022) Continuous counter-current ionic liquid metathesis in mixer- settlers: efficiency analysis and comparison with batch operation. ACS Sustain Chem Eng 10:946–955. https://doi.org/10.1021/acssuschemeng.1c06873
20. Nieva-Echevarría B, Manzanos MJ, Goicoechea E, Guillén MD (2015) 2,6-Di-Tert-Butyl-hydroxytoluene and its metabolites in foods. Compr Rev Food Sci Food Saf 14:67–80. https://doi.org/10.1111/1541-4337.12121
21. Dai S, Yu C, Liang M et al (2023) Oxidation characteristics and thermal stability of butylated hydroxytoluene. Arab J Chem 16:1–10. https://doi.org/10.1016/j.arabjc.2023.104932
22. Yehye WA, Abdul N, Arif A et al (2015) Understanding the chemistry behind the antioxidant activities of butylated hydroxytoluene (BHT): a review. Eur J Med Chem 101:295–312. https://doi.org/10.1016/j.ejmech.2015.06.026